

PROCESS CHARACTERISATION OF PICOSECOND LASER ABLATION OF SiO_2 AND SiN_x LAYERS ON PLANAR AND TEXTURED SURFACES

Sonja Hermann, Tobias Neubert, Bettina Wolpensinger, Nils-Peter Harder, and Rolf Brendel
 Institut für Solarenergieforschung Hameln (ISFH)
 D-31860 Emmerthal, Germany

Severin Massa, Uwe Stute
 Trumpf-Laser GmbH + Co. KG
 D-78713 Schramberg, Germany

ABSTRACT: Local contact openings in dielectric passivating layers of solar cells reduce recombination losses and offer an attractive alternative to “fire-through” processes such as screen printing of grid lines on the front side. Laser ablation with ultra short pulses is particularly suitable for contactless industrial processing of high-efficiency silicon solar cells. In the present paper, we investigate picosecond laser ablation of passivating SiO_2 and SiN_x layers on planar and textured silicon surfaces for various wavelengths of laser radiation. We characterise ps-laser ablated contact openings on 40 - 100 Ω/sq emitters by lifetime and contact resistance measurements. Our results show that for infrared and for visible wavelengths the local emitter saturation current densities in laser treated areas are 1 to 4 pA/cm^2 when ablating SiN_x and SiO_2 layers from planar surfaces. However, ps-laser ablation on alkaline textured surfaces results in server crystal damage. Specific contact resistance values of $< 1 \text{ m}\Omega\text{cm}^2$ are achieved. We characterise the total recombination current densities by measurements of the J - V characteristics of laser treated diodes. Assuming 3% metallised area the efficiency loss compared to wet chemically treated solar cells is very low and amounts to 0.2% absolute.

Keywords: Laser Processing, Selective Ablation, Local Contact Openings, Front Metallisation

1 INTRODUCTION

An efficient strategy for minimising recombination losses of solar cells is to reduce the metal-semiconductor interface area at the contacts and passivating the remaining surface area by dielectric layers. An example of this strategy is the rear side of PERC [1] solar cells where a passivation layer at the rear surface is perforated by local contact openings. Also for developing alternative processes to the established screen printed front side metallisation local contact openings are promising. For obtaining low-cost and highly efficient solar cells, it is crucial to use a reliable technology for realising openings in passivating layers without damaging the underlying silicon. Photolithography, as used in the laboratories to fabricate highly efficient solar cells [2], is not suitable for low-cost mass production. An attractive alternative for industrial production is direct laser ablation of SiN_x and SiO_2 layers that does not require any wet chemical post treatment. There have been reports of ablating UV-absorbing SiN_x layers without appreciable damage to the silicon substrate using nanosecond (ns) laser pulses [3, 4]. We also

demonstrated earlier [5], that the perforation of transparent SiO_2 layers on planar surfaces with ~ 10 ps laser pulses is better controllable and exhibits less damage than when using ns-pulses. Recently, we fabricated a RISE solar cell (4 cm^2 , p-type FZ-Si) that has ps-laser contact openings in the passivating SiO_2 layer on the P-doped emitter as well as on the B-doped back surface field [6]. The high open-circuit voltage of 663 mV as well as the fill factor of 81.5% of this cell indicates the absence of appreciable crystal damage. While these previous experiments focussed on passivating SiO_2 layers using a visible (VIS) wavelength ($\lambda = 532 \text{ nm}$) we compare in this work ps-ablation of SiO_2 -layers in the VIS with ps-ablation in the infrared (IR) spectral range. Additionally we investigate ps-ablation of plasma-enhanced chemical vapour deposition (PECVD) SiN_x layers on planar and textured surfaces. In order to be most sensitive to potential laser-induced crystal damage the main focus of the characterisation of the present work lies on ablating dielectric layers from rather shallow emitters.

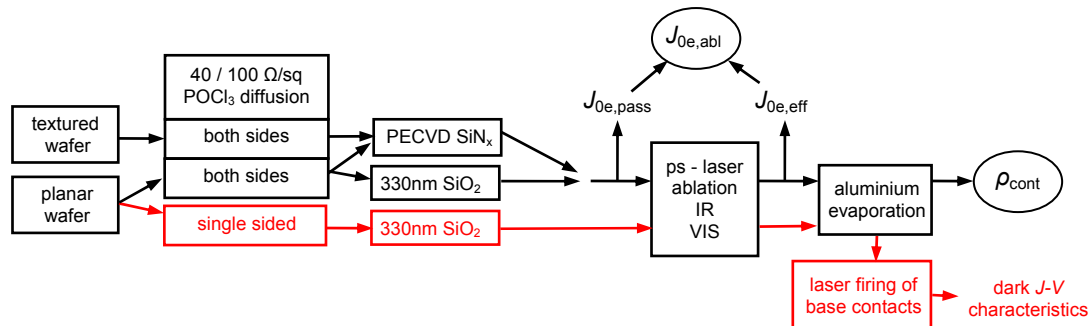


Figure 1: Process scheme of our experiments for the characterisation of ps-laser ablation of SiO_2 and SiN_x layers on P-diffused silicon substrates. We determine local emitter saturation current densities $J_{0e,\text{abl}}$ in laser ablated regions and specific contact resistances ρ_{cont} of metallised samples. Additionally we measure dark J - V characteristics of laser treated diodes.

2 EXPERIMENTAL

We examine the local removal of thermally grown SiO₂ layers (planar samples) and of PECVD SiN_x layers (planar and alkaline textured test structures) from phosphorus-diffused wafer surfaces. In order to characterise whether the removal of the dielectric layer is sufficient for the formation of electrical contacts we measure the specific contact resistance ρ_{cont} of metallised samples. In this work, we apply two methods for quantifying the laser induced crystal damage to phosphorus-diffused silicon substrates. The determination of local emitter saturation current densities $J_{0e,\text{abl}}$ in laser ablated areas enables the characterisation of crystal damage in the emitter bulk and at the surface. Measuring J - V characteristics of laser treated diodes actually detects the impact of the total induced crystal damage, including possible damages in the space charge region and the base volume on the performances of solar cells. The processing sequence of our experiments is shown in Figure 1 and described in detail by the following sections. We use the laser radiation of a Yb:YVO₄ disc laser with a fundamental wavelength of $\lambda = 1030$ nm (IR) and the wavelength of the second harmonic in the VIS range of $\lambda = 515$ nm. The pulse duration of this laser is < 6 ps. We also apply an Nd:YVO₄ slab laser with a pulse duration of 8 to 9 ps also with first (IR, $\lambda = 1064$ nm) and second harmonic radiation (VIS, $\lambda = 532$ nm). For both lasers we apply a single laser shot for ablating the dielectric layers. Thereby we vary the maximal laser fluence Φ_0 [J/cm²], which is defined as the peak energy density in the centre of the Gaussian intensity profile. We also process and measure samples for which the dielectric layer is removed by HF etching. These samples serve as references for the $J_{0e,\text{abl}}$ and ρ_{cont} measurements as well as for the evaluation of the dark J - V curves of the diodes, since wet chemical etching removes the dielectric layers without causing any damage to the silicon crystal.

2.1 Contact resistance measurements

For measuring the specific contact resistance ρ_{cont} we use planar and alkaline-textured phosphorus-diffused, $(1.5 \pm 0.5) \Omega\text{cm}$, p -type FZ-Si wafer with a size of 2.5×2.5 cm². The emitter has a sheet resistance of $40 \Omega/\text{sq}$. We passivate both sides of the wafer with dielectric layers (Fig.1):

- thermal SiO₂ layer on planar samples (1000°C)
- remote-PECVD SiN_x (400°C, $n = 1.9$ (2.1, 2.4)) on planar and textured samples

Subsequently we ablate the dielectric layers on one side of the wafer with a single laser spot per area (that is without pulse overlap) and varying laser fluences. Avoiding pulse overlaps implies that the dielectric layer is not removed from the entire surface area, which has to be taken into account when interpreting the specific contact resistance measurements. After a short cleaning step without any HF treatment we metallise the samples by evaporation of aluminium contact fingers, followed by annealing for 1 minute at 330°C. We extract the specific contact resistance ρ_{cont} of the metal-semiconductor contact by means of the transfer length method [7].

2.2 Local emitter saturation current density

In order to investigate the crystal damage within the emitter we determine the local emitter saturation current densities $J_{0e,\text{abl}}$ in the ablated regions of phosphorus-diffused samples (2.5×2.5 cm²). We use planar and alkaline textured p -type, $(235 \pm 10) \Omega\text{cm}$ FZ-Si wafer and prepare phosphorus-diffused emitters with sheet resistances of 40 and $100 \Omega/\text{sq}$. Subsequently we passivate the wafer as described in the previous section and in Fig. 1. Prior to the laser treatment we measure the injection-dependent effective charge carrier lifetime in high level injection by means of the quasi-steady-state photoconductance method [8, 9]. From the measured effective lifetime we extract the emitter saturation current density for the fully passivated case $J_{0e,\text{pass}}$ as proposed in Ref. [10]. Afterwards, we uniformly ablate the dielectric layers on both sides of the wafer without spot overlap using the same laser parameters as for the contact resistance samples. We then measure the effective lifetime of the samples after laser treatment. The laser ablation of the dielectric layers results in a change of the optical properties of the sample, thus leading to a modified rate of photogeneration. We apply a self-consistent determination of the optical properties by comparing transient and quasi-steady state photoconductance measurements and then extract the emitter saturation current density $J_{0e,\text{eff}}$ from the effective carrier lifetime measurements. $J_{0e,\text{eff}}$ contains contributions from the passivated ($J_{0e,\text{pass}}$) and the laser ablated areas ($J_{0e,\text{abl}}$). We determine the local emitter saturation current density in the ablated areas using the relation $J_{0e,\text{abl}} = [J_{0e,\text{eff}} - (1-f) \cdot J_{0e,\text{pass}}] / f$, where f is the laser-opened area fraction of each sample.

2.3 Dark J - V characteristics of laser treated diodes

The damage inflicted to the sample, including the crystal damage within the p - n junction, becomes apparent in dark J - V curves of ps-laser treated diodes. These diodes display the impact of the laser-induced damage under exactly the conditions relevant for solar cell operation. We prepare diodes with a $40 \Omega/\text{sq}$ emitter, passivated by a thermally grown SiO₂ layer on both sides. Laser ablation without spot overlap creates local contact openings in the SiO₂ layer on the P-diffused side. Choosing a large area fraction f for the contact openings maximises the sensitivity of the experiment for the influence of varying laser parameters. We therefore open the SiO₂ layer on 16 to 64% of the total diode area and then metallise the full area on both wafer sides. The base contacts are formed by laser fired contacts (LFC). The area coverage of the LFC contacts is less than 0.5% in order to minimise their contribution to the total recombination of the diode and thus to maximise the sensitivity for detecting laser-induced crystal damage in the emitter. The samples are annealed for 1 minute at 330°C before measuring the dark J - V curve of the diodes.

3 RESULTS

3.1 Picosecond laser ablation of SiN_x layers

Figure 2 shows the local emitter saturation current densities $J_{0e,\text{abl}}$ in the laser ablated areas (a) as well as the

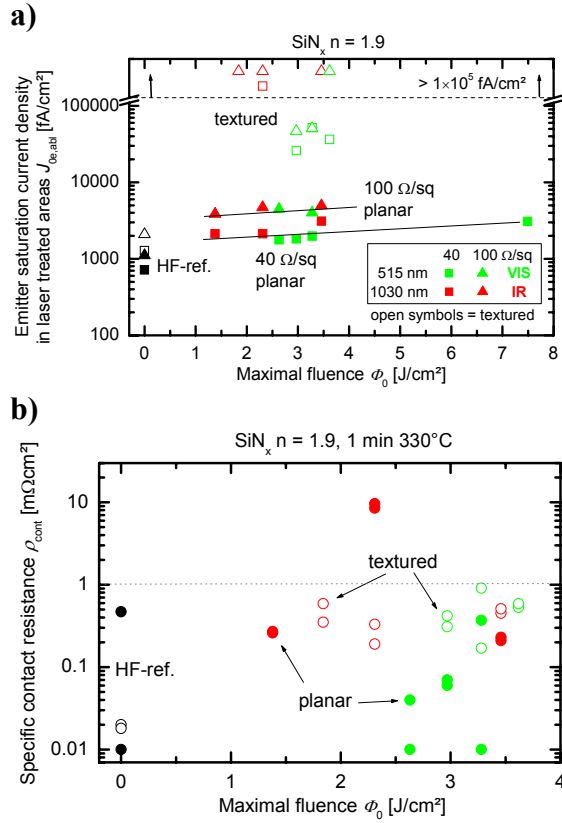


Figure 2: Results of the local ps-laser ablation of SiN_x layers ($n = 1.9$) on planar (solid symbols) and textured surfaces (open symbols). Applied was a Yb:YVO_4 laser with infrared (IR, 1030 nm, red symbols) and visible (VIS, 515 nm, green symbols) wavelength. Plot a) shows the local emitter saturation current densities $J_{0e,abl}$ in the ablated regions on P-diffused 40 Ω/sq and 100 Ω/sq emitters plotted versus the applied maximal laser fluence Φ_0 . Plot b) shows contact resistances on a 40 Ω/sq emitter of accordingly treated samples. HF-reference values (black symbols) are plotted at $\Phi_0 = 0 \text{ J/cm}^2$.

contact resistances ρ_{cont} (b) in the case of SiN_x layer ($n = 1.9$) ablation. Thereby the results are displayed as a function of laser fluence Φ_0 . The plots show results for the infrared (1030 nm, red symbols) and the visible (515 nm, green symbols) wavelength of the Yb:YVO_4 laser for the ablation on planar (solid symbols) and textured (open symbols) samples. The shape of the symbols refers to the sheet resistance of the emitter diffusion. The HF-treated reference samples are denoted by black symbols at $\Phi_0 = 0 \text{ J/cm}^2$. On planar surfaces we achieve local emitter saturation current densities $J_{0e,abl} \approx 2$ to 3 pA/cm^2 which is about three to four times the values of the HF-treated reference samples that have $J_{0e,HF} = 0.7 \text{ pA/cm}^2$. We achieve the same ratio of $J_{0e,abl}/J_{0e,HF}$ in the case of the 100 Ω/sq emitter (triangular symbols) with $J_{0e,abl}$ values of approximately 4 pA/cm^2 . In case of the laser wavelength $\lambda = 515 \text{ nm}$, we find this relatively low level of $J_{0e,abl}$ even at a laser fluence of 7.5 J/cm^2 , which is about three times larger than required for a reliable removal of the SiN_x layer. The $J_{0e,abl}$ values in the range of 1 to 4 pA/cm^2 are well suited for the fabrication of high-efficiency silicon solar

cells. However, using the same wavelength and fluences of 2 to 4 J/cm^2 on textured instead of planar surfaces (open symbols) leads to $J_{0e,abl}$ values of 30 to 60 pA/cm^2 that are thus one to two orders of magnitude higher than the corresponding $J_{0e,HF}$ values. The effective carrier lifetime of these samples does not exceed $10 \mu\text{s}$, which is not acceptable for the fabrication of efficient solar cells. Due to the low lifetime of $< 2 \mu\text{s}$ of some samples we cannot reliably extract their $J_{0e,eff}$ values from the injection dependency of the lifetime as proposed by [10]. We therefore plot these $J_{0e,abl}$ values at above 100 pA/cm^2 without scaling the saturation current density-axis.

The results for ablating SiN_x with a higher refractive index ($n = 2.4$) are virtually identical to those obtained with stoichiometric SiN_x ($n = 1.9$) when using the Yb:YVO_4 as well as the Nd:YVO_4 ps-laser. The findings reported here thus hold for the whole range of refractive indices applied as anti-reflective coatings.

Figure 2b) shows the results of the contact resistance measurements of Yb:YVO_4 laser-ablated samples. The colour and symbol code follows that of Figure 2a). Again solid symbols represent results for planar surfaces and open symbols the results for textured surfaces. We find that the contact resistances ρ_{cont} exhibit values below $< 1 \text{ m}\Omega\text{cm}^2$ (after annealing for 1 min at 330°C) with only one exception for the IR wavelength. The values are therewith very similar to those obtained for the HF-treated references (black symbols). We obtain similar results for the contact resistances when ablating SiN_x by the Nd:YVO_4 ps-laser. Low specific contact resistances enable small metallised area fractions in silicon solar cells. Resistance values of below $1 \text{ m}\Omega\text{cm}^2$ require less than 1% of the total cell area to be contacted. This leads then to a contribution to the series resistance of $< 0.1 \Omega\text{cm}^2$. The ablation of SiN_x layers with refractive index $n = 2.1$ also yields ρ_{cont} values $< 1 \text{ m}\Omega\text{cm}^2$. The ps-laser ablation is therefore well suited to fully remove SiN_x -anti-reflecting coatings from silicon solar cells.

3.2 Picosecond laser ablation of SiO_2 layers

Figure 3a) collects the determined saturation current densities $J_{0e,abl}$ for ablating thermal SiO_2 layers on planar surfaces using the Nd:YVO_4 slab laser. Data set A refers to the laser ablation on a 40 Ω/sq emitter (square symbols) while data set B and C refer to a 55 Ω/sq (circular symbols) and 110 Ω/sq (triangular symbols) emitter, respectively. The colour code is the same as in Figure 2: We mark experiments at $\lambda = 532 \text{ nm}$ in green and those at $\lambda = 1064 \text{ nm}$ in red. The emitter of lighter diffusion (set C) is more sensitive to unpassivated and potentially damaged surfaces and thus shows higher $J_{0e,abl}$ values in the range of 2 to 3 pA/cm^2 . Set B and C obtain $J_{0e,abl}$ values of 1 to 1.5 pA/cm^2 . We find these results to be independent of the laser wavelength. As already seen for the ablation of SiN_x layers (Fig. 2), the $J_{0e,abl}$ values do not show a strong dependence on the laser fluence in a broad fluence range.

However, when applying too high laser fluences of 4 to 5 times the fluence required for reliably opening the passivation layer, then we find local saturation current densities $J_{0e,abl}$ enhancements by up to one order of magnitude indicating severe crystal damage.

Figure 3b) shows the specific contact resistances for ablating SiO_2 layers on a 40 Ω/sq emitter with the Nd:YVO_4 ps-laser. All resistances are $< 1 \text{ m}\Omega\text{cm}^2$ for both wavelengths in a broad range of laser fluence. Only

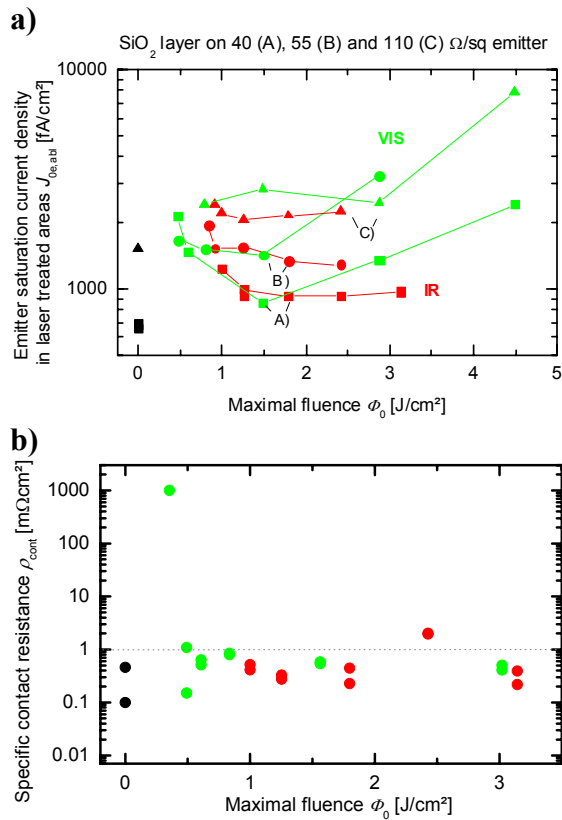


Figure 3: Results of the local ps-laser ablation of thermal SiO₂ layers on planar surfaces. Applied was a Nd:YVO₄ laser with infrared (IR, 1064 nm, red symbols) and visible (VIS, 532 nm, green symbols) wavelength. a): Local diode saturation current densities in ablated regions $J_{0e,abl}$ on P-diffused 40, 55 and 110 Ω/sq emitters plotted versus the applied maximal laser fluence Φ_0 . b) Contact resistances on a 40 Ω/sq emitter of accordingly treated samples. HF-reference values (black symbols) are plotted at $\Phi_0 = 0 \text{ J/cm}^2$.

for fluences below 0.5 J/cm^2 , we find an increase of contact resistance. At this low pulse energy the oxide layer is not fully ablated. This effect also occurs for

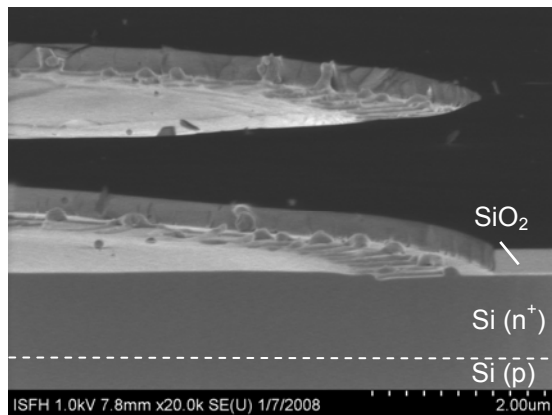


Figure 4: Scanning electron microscope image of local contact openings in a 330 nm thermal SiO₂ layer realised by direct ps-laser ablation.

corresponding experiments with the Yb:YVO₄ ps-laser (not shown in Fig. 3). Figure 4 shows a scanning electron micrograph of openings in a thermal SiO₂ layer, created by ps-laser ablation. We find only minor surface modifications well above the p - n junction that is approximately 0.9 μm deep as indicated by the dashed line. However, electronically active crystal defects such as in the n^+ -region or the p - n junction region are in general not detectable from such micrographs.

The current-voltage (J - V) curve of a diode is a very sensitive tool for detecting recombination due to such defects. While this recombination can be highly detrimental for the fill factor of solar cells, it is not detected by measuring the emitter saturation current density discussed in the previous paragraphs.

Figure 5 shows measured dark J - V curves of diodes with a 40 Ω/sq emitter, treated with 532 nm radiation of the Nd:YVO₄ laser at fluences Φ_0 ranging from 0.6 to 4.5 J/cm^2 . The curve of the HF-treated reference diode is marked with $\Phi_0 = 0 \text{ J/cm}^2$ and plotted in black symbols. Note that reverse currents are plotted as positive values. The various diodes differ in the laser treated and metallised emitter surface fraction f that ranges from 100% for of the HF reference to 16 to 64% for the laser treated samples. The dashed lines in Fig. 5 give the slope for the ideality factors $n=1$ and $n=2$. Within the voltage range of the expected maximum power point (0.5 to 0.6 V) the laser-treated samples have an ideality factor of about $n \approx 2$. We therefore conclude that the emitter saturation current densities as shown in Fig. 3a) give only an incomplete characterisation of the recombination losses due to the laser-induced damage.

Hence, we apply the following procedure for assessing the impact of the laser damage on the diodes: We assume that the base volume including rear side recombination is modelled with a saturation current of

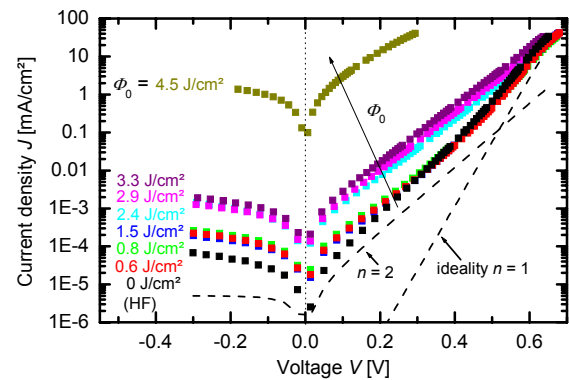


Figure 5: Measured dark J - V curves of ps-laser treated diodes. Applied was a Nd:YVO₄ laser with the wavelength of 532 nm at varying laser fluences Φ_0 from 0.6 to 4.5 J/cm^2 . Both sides of the diodes are passivated by a thermal SiO₂ layer. The emitter is contacted via the uniformly applied local laser contact openings with an intentionally high contacted area fraction of 16 to 64 %. Front and rear side of the diodes are fully metallised and the base is contacted via laser-fired contacts (LFC). The J - V curve of the chemically treated reference diode (emitter metallisation area fraction $f = 100\%$) is plotted in orange symbols. For each curve, the first and second fitting diodes are additionally plotted in lines of the accordant colour.

$J_{0b} = 100 \text{ fA/cm}^2$. The saturation current density of the passivated emitter is $J_{0e,pass} = 60 \text{ fA/cm}^2$. We subtract this “background recombination” from the measured J - V curves $J_{diode}(V)$ to obtain the recombination current

$$J_{cont}(V) = \frac{1}{f} \left[J_{diode}(V) - (J_{0b} + (1-f) \cdot J_{0e,pass}) \cdot \left(e^{\frac{qV}{k_B T}} - 1 \right) \right]$$

that is due to the contacted emitter. Here f is the area fraction of contacted openings on our diodes.

We now assess the impact of this contact recombination $J_{cont}(V)$ onto the performance of solar cells. Our hypothetical “baseline solar cell” has without any recombination at the emitter contacts a lumped saturation current density of $J_0 = 150 \text{ fA/cm}^2$, a short circuit current density of 40 mA/cm^2 and a series resistance of $1 \text{ } \Omega\text{cm}^2$. This set of parameters leads to an efficiency of 21.3% as indicated by the uppermost dashed line in Figure 6. In order to simulate the impact of contact recombination we add an additional recombination of $0.03 \times J_{cont}(V)$ to the recombination of the baseline solar cell. This corresponds to a metallised area fraction of 3%.

The black dashed line in Figure 6 displays the calculated efficiency representing 3% of wet chemically produced contacts openings, while the green symbols represent the calculated efficiencies for laser-opened contacts. The highest efficiency achievable for the baseline cell with contact openings made by ps-laser ablation is only 0.15% absolute lower than the efficiency achievable by wet chemically opened contacts. Within a wide fluence range from 1 to 3 J/cm^2 the efficiency loss is less than 0.25% absolute. Increasing the laser fluence beyond a value of 3 J/cm^2 leads to drastically enhanced efficiency losses.

Interestingly, for very low laser fluences we also find efficiency losses due to enhanced recombination. This is in good qualitative agreement to what we observe for the emitter saturation current densities in Fig. 3a).

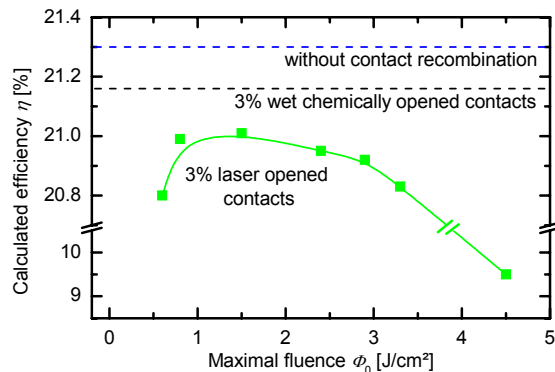


Figure 6: Calculated solar cell efficiencies with impact of recombination losses due to contact openings made by 532 nm ps-laser ablation. The voltage dependent recombination under the contacts is based on the measured J - V curves shown in Figure 6.

4 CONCLUSIONS

This work characterises laser-induced damage generated when ablating of SiO_2 and SiN_x layers from phosphorus-diffused emitters. For planar surfaces we find

that at laser fluences $< 3 \text{ J/cm}^2$ the ps-laser ablation allows to produce contact openings in the dielectric layer with series resistances $< 1 \text{ m}\Omega\text{cm}^2$ and only minor degree of crystal damage. The choice of the laser wavelength (IR or VIS) does not significantly affect the emitter saturation current as deduced from lifetime measurements. Furthermore, we find that the ps-laser ablation causes severe crystal damage on alkaline texture-etched surfaces.

Evaluating J - V characteristics of SiO_2 passivated and laser ablated diodes we find that the laser induced damage causes recombination currents with ideality factors around 2, which potentially affect the fill factor of solar cells. Assuming 3% metallised area for a solar cell we estimate from model calculations that within a broad laser fluence range from 1 to 3 J/cm^2 the efficiency loss due to the laser treatment amounts to approximately 0.2% absolute when compared to wet chemically treated solar cells. This broad process window in the case of ps-laser ablation from planar surfaces is attractive for setting up a reliable industrial process for high-efficiency solar cells.

5 ACKNOWLEDGEMENTS

Funding was provided by the State of Lower Saxony and the German Federal Ministry for the Environment, Nature Conservation and Nuclear Safety (BMU) under contract No 0327547A.

6 REFERENCES

- [1] A.W. Blakers, A. Wang, A.M. Milne, J. Zhao, M.A. Green, *Applied Physics Letters* **55**, 1363 (1989).
- [2] J. Zhao, A. Wang, M.A. Green, *Progress in Photovoltaics* **7**, 471 (1999).
- [3] P. Engelhart, N.-P. Harder, T. Horstmann, R. Grischke, R. Meyer, R. Brendel, in *Proc. 4th World Conference Solar Energy Conversion*, (Hawaii, 2006) p. 1024.
- [4] A. Knorz, A. Grohe, C. Harmel, R. Preu, J. Luther, in *Proc. 22nd European Photovoltaic Solar Energy Conference* (Milan, 2007) p. 1488.
- [5] P. Engelhart, S. Hermann, T. Neubert, H. Plagwitz, R. Grischke, R. Meyer, U. Klug, A. Schoonderbeek, U. Stute, R. Brendel, in *Progress in Photovoltaics: Research and Applications* **15**, 521 (2007).
- [6] S. Hermann, P. Engelhart, A. Merkle, T. Neubert, T. Brendemühl, R. Meyer, N.-P. Harder, R. Brendel, in *Proc. 22nd European Photovoltaic Solar Energy Conference* (Milan, 2007) p. 970.
- [7] C.L. Meier, D.K. Schroder, *IEEE Transactions on Electron Devices* **31**, 647 (1984).
- [8] A. Cuevas, M. Stocks, D. Macdonald, R. Sinton, in *Proc. 2nd World Conference Solar Energy Conversion* (Vienna, 1998) p. 1236.
- [9] H. Nagel, C. Berge, A. G. Aberle, *Applied Physics Letters* **86**, 6218 (1999).
- [10] D.E. Kane, R.M. Swanson, in *Proc. 18th IEEE Photovoltaic Specialists Conference* (IEEE, New York, 1985) p. 578.